Tooth Contact Shift in Loaded Spiral Bevel Gears

Michael Savage, University of Akron, Akron, OH
P.C. Altidis, Clark Material Handling Co., Lexington, KY
D. G. Lewicki & J. J. Coy, NASA Lewis Research Center, Cleveland, OH
F. L Litvin, University of Illinois at Chicago, Chicago, IL

Nomenclature

a Tooth mid-cone plane addendum, m
A Distance from gear to first bearing, m
A_0 Outer-cone distance, m
B Distance from gear to second bearing, m
D Tooth contact shift, m
D_0 Mid-cone distance, m
EI Elastic support stiffness, N-m^2
EI_0 Elastic support stiffness of base design, N-m^2
f Tooth face width, m
N Number of teeth
O Center of curvature
p_b Base pitch equivalent spur gear, m
r Mid-plane pitch radius, m
R Mid-cone pitch radius, m
R_e Effective pitch radius, m
R'_e Loaded effective pitch radius
T Torque, N-m
U Pitch point tangential motion, m
W Force component, N
X Bearing radial deflection, m
Y Pitch point deflection, m
Z Gear center deflection, m
β Orthogonal coordinate frame
Γ Cone angle, rad
θ Pitch point slope, rad
ρ Radius of curvature, m
Σ Shaft angle, rad
ϕ_n Normal pressure angle, rad
ϕ'_n Loaded normal pressure angle, rad
ψ Spiral angle, rad

Subscripts

a Axial first bearing
b Second bearing
bi, i = 1, 2, 3 motion from bearing in first coordinate frame direction
ci, i = 1, 2, 3 motion from shaft in first coordinate frame direction
di, i = 1, 2, 3 first coordinate frame direction
ei, i = 1, 2, 3 second coordinate frame direction
fi, i = 1, 2, 3 third coordinate frame direction
gi, i = 1, 2, 3 fourth coordinate frame direction
g Gear (as last subscript)
p Pinion (as last subscript)
r Radial
t Tangential

Abstract: An analytical method is presented to predict the shifts of the contact ellipses on spiral bevel gear teeth under load. The contact ellipse shift is the motion of the tooth contact position from the ideal pitch point to its location under load. The shifts are due to the elastic motions of the gear and pinion supporting shafts and bearings. The calculations include the elastic deflections of the gear shafts and the deflections of the four shaft bearings. The method assumes that the surface curvature of each tooth is constant near the unloaded pitch point. Results from these calculations will help designers reduce transmission weight without seriously reducing transmission performance.

Introduction

Spiral bevel gears are important elements for transmitting power. In designing spiral bevel gear transmissions, the designer meets a tradeoff between a transmission's weight and its life and reliability. By removing weight from transmission components, one increases the overall flexibility of the transmission. This flexibility affects the deflections of the loaded components in the transmission.

The design of an efficient spiral bevel gear box includes the design of gear and support geometry, bearing and shaft sizes, and material properties. The gear tooth interaction is more complex than that of spur or helical gears. The loaded region of the gear mesh shifts due to the deflections of the gear and the pinion. A primary cause of these motions is the flexibility of the gear support shaft and bearings. Although the teeth also deflect, tooth beam deflections are small in comparison to tooth gear support deflections. If

the shift of the loaded region is large, the life of the gear mesh may reduce significantly.

The classic work of Wildhaber[1-2] describes the kinematic operation and the generation of spiral bevel gears. More recently, Baxter[3] and Coleman[4] expanded on this fundamental theory. They described a tooth contact analysis program which analyzes the kinematic action of two spiral bevel gears in mesh. The program considers effects of tooth manufacturing parameters on the gear mesh kinematics.

Litvin and Coy[5] and Litvin, Rahamn and Goldrich[6] also presented the theory of spiral bevel gear generation and design. These works describe kinematic errors induced in the transmission by errors in gear manufacturing and assembly. The articles also suggest tooth profile modifications to improve kinematic transmission. They give direct relationships for the generated curvatures and directions on the terms of the principal curvatures and directions on the bevel gear teeth surfaces. These relationships are in terms of the principal curvatures and directions of the tool generating surfaces.

Coleman[7] described the experimental measurement of existing bevel and hypoid gear deflections under load. The article cites the importance of these deflections for the capacity and noise level of the gear set. The test results also suggest gear mounting and tooth manufacturing changes which can improve the capacity and life of the gear set.

Taha, Ettles, and MacPherson[8] presented the interaction of the structural rigidity and performance from a helicopter tail rotor gear box. They used a finite element model for the housing. The article presents effects of deflections on bearing roller load distribution, bearing fatigue life, and the gear motions at the unloaded pitch point. Their work demonstrates the importance of rigidity to minimize deflections and maximize bearing life in a transmission.

Winter and Paul[9] presented work on the influence of spiral bevel gear deflection on tooth root stresses.

This article presents an analytical method to predict the shift of the loaded region on the tooth. The method treats the shift as a result of the elastic deflections of the gear support shafting and bearings. The analysis is sequential.

The first stage defines the gear geometry and loading. The second stage determines the elastic deflections of the bearings and shafts and the slopes of the shafts at the gears. The third stage finds the motions of the gear teeth caused by each elastic deflection. The total deflections of the gear teeth are the algebraic sum of these motions. The fourth stage determines the geometry and curvatures of the gear and pinion teeth. These directions and curvatures combine with the separate motions of the gear teeth to produce the contact shift. The contact shift is the motion of the contact ellipses on the two tooth surfaces under load from the unloaded pitch point. The analysis assumes that the curvatures are constant over the affected surfaces of the teeth.

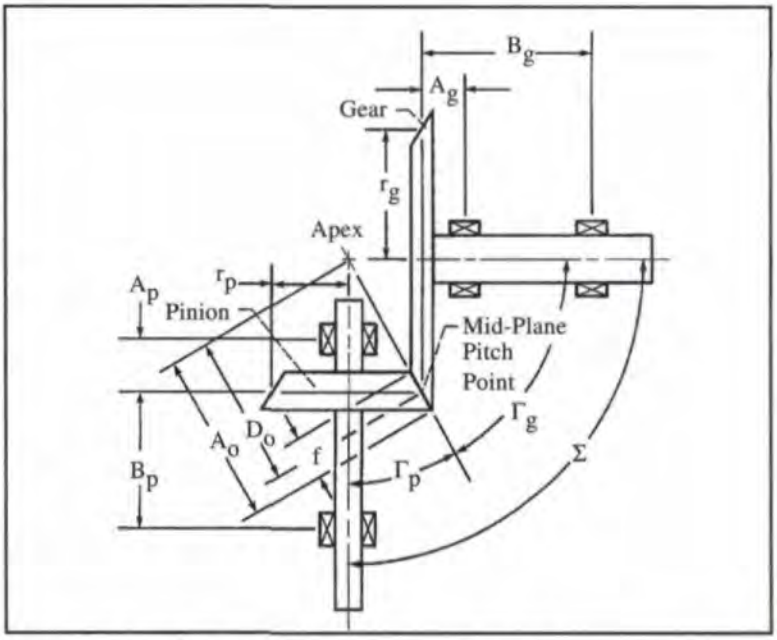

Fig. 1 - Spiral bevel gear mesh and support bearing geometry.

A gear box model similar to the main rotor bevel gear reduction of the U.S. Army OH-58 light duty helicopter serves as an example for the method. The gear box includes a single spiral bevel gear drive with a pinion input and the supporting shafts and bearings. The analysis includes a parametric study. The article presents radial and tangential shifts of the contact ellipses on the pinion and gear teeth as functions of shaft stiffness.

Geometry and Loading

Fig. 1 shows the geometry of a spiral bevel gear mesh. The mid-cone distance, D_o, is the distance from the apex of the bevel cones to the mid-place pitch point. This distance is along the pitch line of the two pitch cones. It is equal to the outer-cone distance, A_o, minus one-half the tooth face width, f. The mid-cone distance and the tooth face width describe the basic gear blank sizes. The cone pitch angles, Γ_g and Γ_p, for the

Michael Savage
is Professor of Mechanical Engineering at the University of Akron, Akron, OH.

P. C. Altidis
is a Senior Design Engineer at Clark Material Handling Company, Lexington, KY.

D. G. Lewicki
is a Research Engineer and at NASA Lewis Research Center, Cleveland, OH.

Dr. J. J. Coy
is the Chief of the Mechanical Systems Branch at NASA Lewis Research Center, Cleveland, OH.

Dr. F. L. Litvin
is on the faculty of the Mechanical Engineering Dept. at the University of Illinois at Chicago.

gear and pinion also contribute to the gear sizes. The shaft angle, Σ, is the sum of the cone pitch angles. The shaft angle defines the relative orientation of the gear and pinion shafts. The pitch radius of the gear in its mid-line, r_g is:

$$r_g = D_o * sin\ \Gamma_g \quad (1)$$

The cone pitch angle, Γ_g, in terms of the numbers of teeth on the gear and pinion, N_g and N_p, and the shaft angle, Σ, is:

$$tan\ \Gamma_g = \frac{sin\ \Sigma}{(N_p/N_g) + cos\ \Sigma} \quad (2)$$

Similar equations define the pitch radius, r_p, and cone pitch angle, Γ_p, of the pinion with the subscripts p and g interchanged.

Fig. 2 shows the spiral angle, ψ, and normal pressure angle, ϕ_n. The spiral angle, ψ, is the angle of inclination of the teeth to the pitch ray. It is in the place tangent to the two pitch cones. The gear of Fig. 2 has a right hand spiral. The normal pressure angle, ϕ_n, is the angle between a normal to the tooth and the tangent to the pitch cone surface in the tooth normal plane.

Fig. 2 includes four orthogonal right handed coordinate frames. All four coordinate frames are at the mid-plane pitch point of the spiral bevel tooth. The first of these, β_{di}, has coordinates in the tangential, axial, and radial directions of the gear body. The second coordinate frame, β_{ei}, is the first coordinate frame rotated through the cone angle, Γ_g, in a negative direction about the β_{d1} vector. The unit vectors of this frame are in the tangential, pitch ray, and mid-cone radial directions, respectively. The third coordinate frame, β_{fi}, is the second coordinate frame rotated through the spiral angle, ψ, in a positive direction about the β_{e3} vector fora right handed spiral angle. The unit vectors of this frame are tangent to the pitch cone in the tooth normal place, tangent to the tooth in the cone tangent plane, and in the mid-cone radial direction respectively. The fourth coordinate frame, β_{gi}, is the third coordinate frame rotated through the normal pressure angle, ϕ_n, in a negative direction about the β_{f2} vector. The unit vectors of this frame are in the tooth normal direction, tangent to the tooth in the cone tangent plane, and tangent to the tooth in the tooth normal plane respectively.

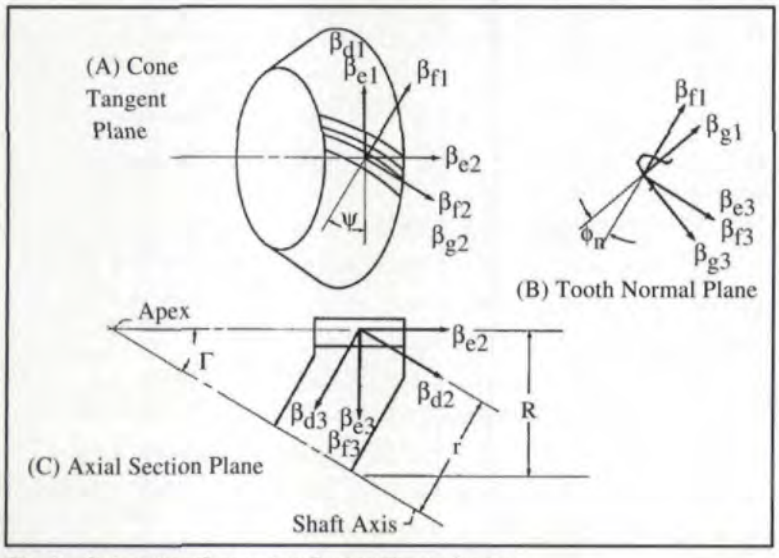

Fig. 2 - Spiral bevel gear tooth coordinate frames.

Fig. 2 shows the mid-plane pitch radius of the gear, r_g, in the axial section plane. The mid-cone radius of the gear, R_g, is in the same view.

This equivalent spur pitch radius is:

$$R_g = \frac{r_g}{cos\ \Gamma_g} \quad (3)$$

The gear assembly includes the support bearings and their locations. The position of the bearings relative to the gear or pinion describes the support system geometry. The two most common bearing configurations are straddle and overhung mountings. Fig. 1 shows both. The pinion has a straddle mounting, while the gear has an overhung mounting. In both cases, A is the distance from the gear mid-plane to the bearing closest to the pitch cone apex. B is the distance from the gear mid-plane to the bearing furthest from the apex. Distance A is positive for an overhung mounting and negative for a straddle mounting. B is always positive.

The normal force acts on the tooth at the mid-plane pitch point. The method assumes that the force is a concentrated force. The force has three orthogonal components in the directions of the β_{di} coordinate frame relative to the tooth. The tangential component, W_t, produces the torque on the gear. It acts in the β_{d1} direction. The axial component, W_a, acts in the β_{d2} direction. And the radial component, W_r, acts in the β_{d3} direction.

Fig. 3 shows these forces for both the gear and the pinion with their respective coordinate frames. For the gear, the components are:

$$W_t = \frac{T_g}{D_o * sin\ \Gamma_g} \quad (4)$$

$$W_a = \frac{|W_t|}{\cos \psi} [\tan \phi_n * \sin \Gamma_g + \sin \psi * \cos \Gamma_g] \quad (5)$$

$$W_r = \frac{|W_t|}{\cos \psi} [\tan \phi_n * \cos \Gamma_g - \sin \psi * \sin \Gamma_g] \quad (6)$$

where T_g is the torque on the gear. Replacing the subscript g with the subscript p in Equations 4 through 6 gives the equations for the pinion force components. In Equations 5 and 6, the sign of the last term depends on the direction of rotation, the hand of the spiral, and whether the gear is driving or being driven. These equations are valid for a right-handed spiral driving gear rotating counterclockwise about the β_{d2} direction. Each change in the spiral hand, power direction, or rotation direction reverses the signs.

The sign of the tangential load, W_t, also depends on the directions of the rotation and power flow. The tangential component is positive for a driving gear or pinion which is rotting counterclockwise. It is also positive for a driven gear of pinion which is rotating clockwise. The tangential load is negative otherwise. However, Equations 5 and 6 use the absolute value of W_t.

Component Deflections

Under load, the motion of the ideal pitch point of a spiral bevel gear is mainly the superposition of three elastic deflections. These deflections result from shaft deflections at the gear centers, shaft slopes at the gear centers, and the deflections of the support bearings.

Table I lists the results of a strength of materials shaft analysis for the deflections, Y_{ci}, and slopes (rotations), ϕ_{ci}, of the gear at the pitch point in and about the β_{di} directions. In the analysis, both the axial and radial forces contribute to both the radial deflection and the tangential rotation. The axial deflection is due to the tangential rotation and the radial location of the pitch point. In this instance, the straddle and overhung cases require different formulae due to the different elastic configurations of the two cases. As before, interchanging gear and pinion subscripts yields valid equations for the pinion.

The bearings which support the shaft also deflect. Each bearing has a nonlinear stiffness and its own contact angle. Harris[10] and Houghton[11] present methods for determining the rolling element load sharing and resulting deflection. The method of this article combines the radial and axial loads on each bear-

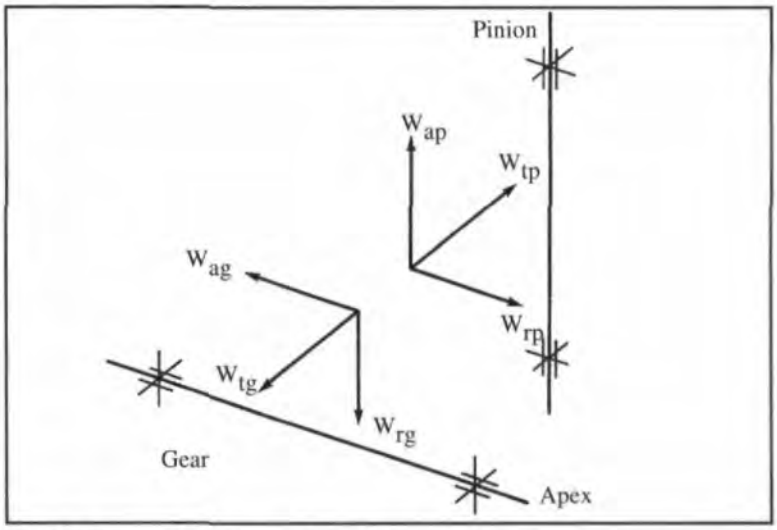

Fig. 3 - Gear and pinion tooth force components.

DEFLECTIONS	
Straddle	Overhung
$Y_{c1} = \frac{W_t A^2 B^2}{3 EI (B-A)}$	$\frac{W_t A^2 B}{3 EI}$
$Y_{c2} = r * \theta_{cl}$	$r * \theta_{cl}$
$Y_{c3} = \frac{-W_a r AB(B + A)}{3 EI (B-A)} + \frac{W_r A^2 B^2}{3 EI (B-A)}$	$\frac{-W_a r A (2B + A)}{6 EI} + \frac{W_r A^2 B}{3 EI}$
SLOPES	
$\theta_{c1} = \frac{W_a r (A^2 + AB + B^2)}{3 EI (B-A)} - \frac{W_r AB (B + A)}{3 EI (B-A)}$	$\frac{W_a r (2A + B)}{3 EI} - \frac{W_r A(2B + A)}{6 EI}$
$\theta_{c2} = 0$	0
$\theta_{c3} = \frac{W_t AB(B + A)}{3 EI (B-A)}$	$\frac{W_t A(2B + A)}{6 EI}$

Table 1 - Elastic Support Induced Pitch Point Motion

DEFLECTIONS
$y_{b1} = \frac{B * X_{a1} - A * X_{b1}}{B - A}$
$y_{b2} = X_2 + r * \theta_{b1}$
$y_{b3} = \frac{B * X_{a3} - A * X_{b3}}{B - A}$
SLOPES
$\theta_{b1} = \frac{X_{b3} - X_{a3}}{B - A}$
$\theta_{b2} = 0$
$\theta_{b3} = \frac{X_{a1} - X_{b1}}{B - A}$

Table 2 - Bearing Induced Pitch Point Motion

ing to find the bearing deflections. The program then resolves each bearing deflection into its radial and axial components in the β_{di} coordinate directions.

The deflections at the bearings are X_{ai} and X_{bi}. Here the subscript a identifies the bearing located the distance A from the gear. And the subscript b identifies the bearing located the distance B away. The last subscript, i, denotes the deflection direction in the β_{di}coordinate frame.

For $i = 2$, both bearings have the same axial deflection, X_2. Table II lists the deflections, Y_{bi}, and the rotations, β_{di} of the gear pitch point caused by these bearing deflections. The motions are due to the rigid body motion of the gear and support shaft in the bearings.

The total motions of the gear pitch point in and about the θ_{di} coordinate directions, neglecting any elastic motion of the transmission housing are:

$$Y_{di} = Y_{bi} + Y_{ci} \text{ for } i = 1, 2, 3 \qquad (7)$$

$$\theta_{di} = \theta_{bi} + \theta_{ci} \text{ for } i = 1, 2, 3 \qquad (8)$$

Similar equations describe the motion of the pinion pitch point. The motions of the gear and pinion pitch points combine in the analysis for the shift of the contact ellipse under load.

Contact Analysis

The principal curvatures of the teeth are needed in addition to the teeth deflections in the contact ellipse shift model. Unfortunately, no direct equations exist for the spiral bevel tooth surface due to the complexity of the surface geometry[5-6]. However, an indirect approach can determine the principal curvatures and directions of curvature. Litvin[5-6] has developed equations to determine these principal curvatures and their directions at the pitch point.

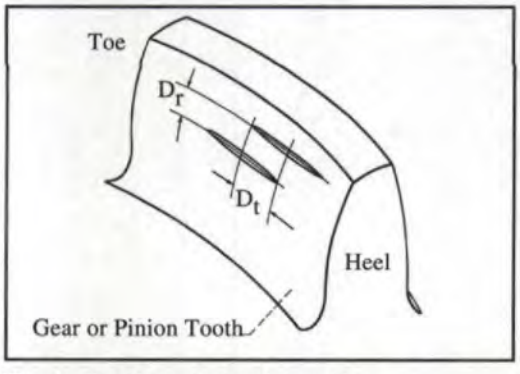

Fig. 4 - Tooth contact point motion.

The analysis assumes that direct conjugate relationships exist between the gear cutting tool surface curvatures and motion and the sought quantities. These are the principal curvatures and their directions on the gear tooth surface. The analysis uses the gear and pinion geometry along with the cutter machine settings for both the gear and pinion. The cutter machine's manufacturer provides the gear cutter settings. With this method, one can determine the curvatures of the gear tooth surface without equations for the surface.

The separate pitch point motions of the two gear teeth effect the shift of the contact ellipse under load. In addition, the motions of the centers of transverse curvature of the teeth surfaces effect the tangential contact ellipse shift. The motions of the mid-plane base circles of the teeth also effect the radial contact ellipse shift. In addition, the standard Hertzian contact stress formulae[12] yield the size and orientation of the contact ellipse on the gears. All these calculations assume that the principal curvatures remain constant over the contacted portions of the spiral bevel gear teeth.

Relative Motions

The contact shift motion occurs in the plane tangent to the two teeth. Relative motions in the direction of the common normal to the teeth produce kinematic errors in the motion transmission. Kinematic error[5] is a forward or backward rotation of the output gear from its ideal position relative to the input gear. This motion does not produce a shift of the contact ellipse. Only the radial shift on the teeth in the tooth normal plane and the tangential relative motion in the cone tangent plane are of interest. The radial shift of the teeth produces a radial shift in the contact ellipse locations on both teeth. The tangential motion produces a tangential shift in the contact ellipse locations as shown in Fig. 4.

In the motion analysis, the small pitch point deflections and rotations are vectors. One can obtain the vector components in any of the four coordinate frames by direct matrix rotations.

Radial Shift - The radial shift of the two teeth appears in the mid-cone plane and in the tooth normal plane. Fig. 5 shows two equivalent spur gears in the tooth normal plane before and after application of the separating load. Equivalent spur gears have the tooth geometry of the spiral bevel tooth in its mid-cone plane. The involute

action of these spur gears is the same as that of spiral bevels in the mid-cone plane.[1-3] The radial shift of the two gears is due to an increase of the center distance in this rotated mid-cone plane. The separating motion of each gear center is the pitch point motion in the β_{e3} direction minus a small relative motion. The relative radial motion of the gear center is toward the pitch point. It is due to the gear rotation about the original tangential direction β_{e1}.

The displacement of the pitch point in the β_{e3} direction is:

$$Y_{e3,g} = Y_{d2,g} * \sin \Gamma_g + Y_{d3,g} * \cos \Gamma_g \quad (9)$$

The effective radius of the equivalent spur gear in the tooth normal plane, R_{eg}, is a function of the mid-cone radius, R_g, and the spiral angle, ψ:

$$R_{eg} = \frac{R_g}{\cos^2 \Psi} \quad (10)$$

The motion of the center of the equivalent gear is thus:

$$Z_{e3,g} = Y_{e3,g} - R_{eg}(1.0 - \cos \theta_{d1,g}) \quad (11)$$

Due to the involute action on separation, the radial motion produces a new loaded pitch point. The normal pressure angle increases slightly. The gears rotate slightly, and a new loaded effective pitch radius results. The new pressure angle, θ'_n, is:

$$\phi'_n = \cos^{-1}\left[\frac{(R_{eg} + R_{ep}) * \cos \phi_n}{R_{eg} + Z_{e3,g} + R_{ep} + Z_{e3,p}}\right] \quad (12)$$

The loaded effective gear pitch radius, R'_{eg}, is:

$$R'_{eg} = \frac{R_{eg} * \cos \phi_n}{\cos \phi'_n} \quad (13)$$

The radial shift of the pitch point from the unloaded to the loaded position on the gear tooth, D'_{rg}, is now:

$$D_{rg} = \frac{R'_{eg} - R_{eg}}{\cos \phi_n} \quad (14)$$

Fig. 6 shows this shift distance and the two pitch radii. Fig. 6 is a normal view of the spiral bevel gear tooth. The analysis for the radial shift of the contact point on the pinion tooth is similar.

Tangential Shift - The relative tangential motion of the two teeth appears clearly in a plane normal to the tooth. This plane contains the tooth tangent vector β_{g2}. The plane is perpendicular to vector β_{g3}. It contains the tangential motion of the pitch points, and it contains the centers of transverse curvature of the gear and pinion teeth, O_g and O_p respectively. The radii of transverse curvature of the teeth, ρ_g and ρ_p, are primary curvatures which the tooth contact analysis determines.

Fig. 7 shows the line of centers in this plane for both the unloaded and the loaded condition. The centers of curvature, O_g and O_p, have a prime in their loaded positions. For clarity, the two centers of curvature are on opposite sides of the tooth surface tangent in Fig. 7. In reality, both centers are on the same side of the tooth surface tangent. However, the tangent shift relation is the same for both cases. The deflections of these centers of curvature in this plane are related to their respective pitch point deflections in the β_{g3} direction. The relation adds the motion of the curvature center relative to the original pitch

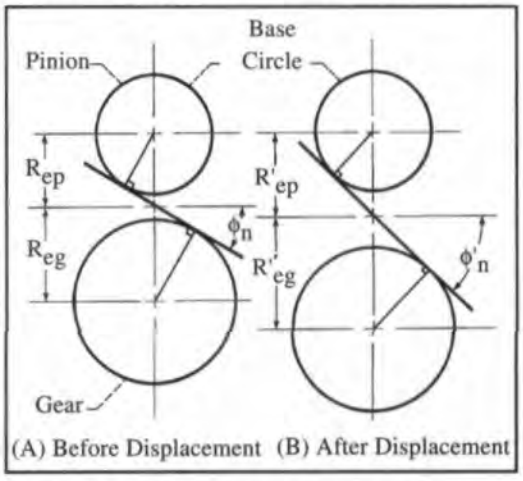

Fig. 5 - Equivalent spur gear separation in tooth normal plane.

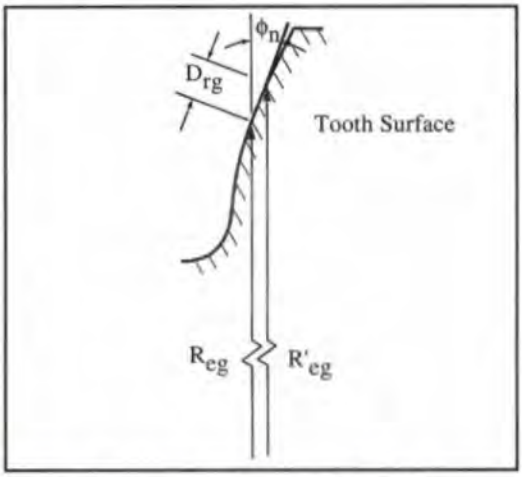

Fig. 6 - Radial motion of gear pitch point.

point. The relative motion is due to the gear body rotation perpendicular to this plane about the β_{g3} direction. For the gear, this deflection is:

$$Z_{g2,g} = Y_{g2,g} + \rho_g * \sin \theta_{g3,g} \quad (15)$$

where

$$Y_{g2,g} = -Y_{d1,g} * \sin \psi + Y_{d2,g} * \cos \Gamma_g \cos \psi - Y_{d3,g} * \sin \Gamma_g \cos \psi \quad (16)$$

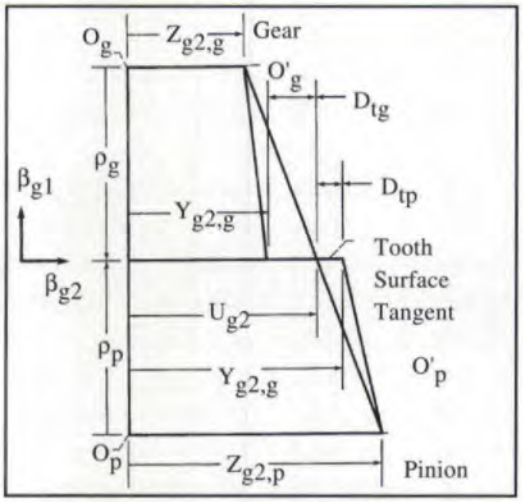

Fig. 7 - Tangential motion of spiral bevel pitch point.

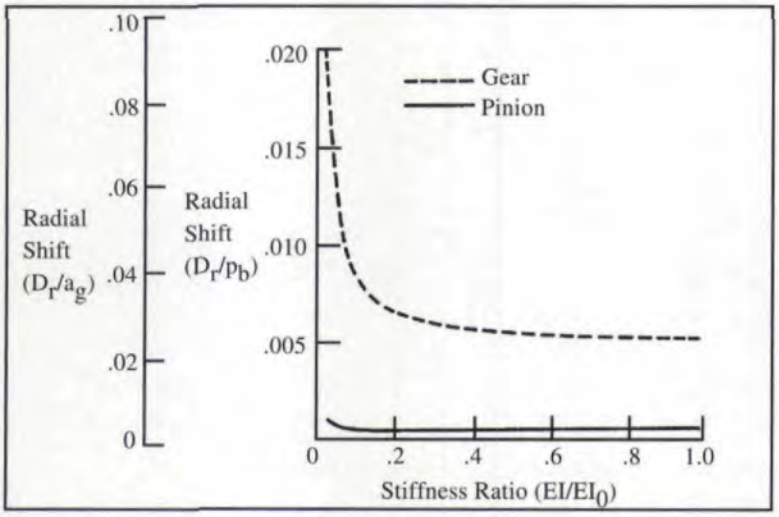

Fig. 8 - Tooth contact position shift in radial direction.

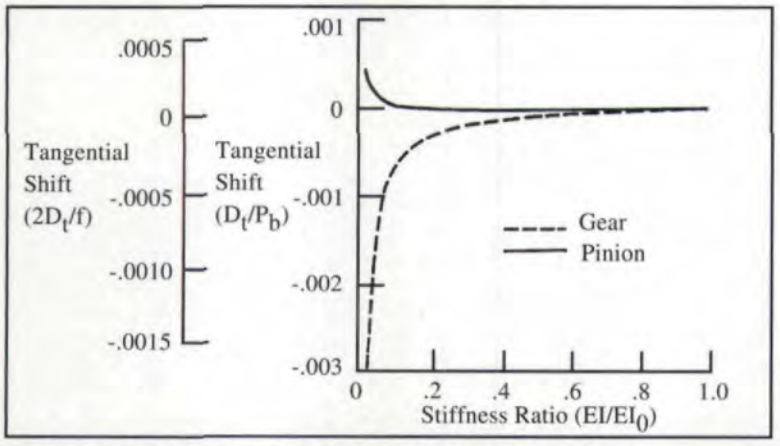

Fig. 9 - Tooth contact position shift in tangential direction.

and:

$$\theta_{g3,g} = \theta_{d1,g} * \cos \psi \sin \phi_n + \theta_{d2,g} * (\cos \Gamma_g \sin \psi \sin \phi_n - \sin \Gamma_g \cos \phi_n) - \theta_{d3,g} * (\sin \Gamma_g \sin \psi \sin \phi_n + \cos \Gamma_g \cos \phi_n) \quad (17)$$

The motion on the tooth surface from the unloaded pitch point to the loaded pitch point in this plane is U_{g2}. This is the deflection necessary to keep the centers of curvature on a common tooth normal.

$$U_{g2} = Z_{g2,g} \frac{\rho}{\rho} + \frac{g}{g + \rho_p} (Z_{g2,p} - Z_{g2,g}) \quad (18)$$

This locates the new loaded pitch point relative to the unloaded pitch point. The relative shift of the gear pitch point in the tangential direction on the tooth surface is D_{tg}. This is the difference between the original pitch point's motion and the pitch point shift, U_{g2}:

$$D_{tg} = U_{g2} - Y_{g2,g} \quad (19)$$

A similar analysis determines the tangential pitch point shift on the pinion, D_{tp}.

Tooth Contact Shift

The radial and tangential components of tooth contact shift are valuable measures of the rigidity of a bevel gear mesh. Knowledge of the shift components can help a designer evaluate important properties of the gear mesh and support bearings. An interactive input Fortran 77 computer program[13] calculates these tooth contact shifts for both the gear and pinion. The program, SLIDE.FOR, can run on a personal computer.

Fig. 4 shows the shift of the nominal pitch point contact ellipse on a gear tooth. The principal radii of curvature of the teeth and the normal tooth load determine the size and orientation of the contact ellipse. One can compare the tangential shift to the difference between the half tooth width and the tangential radius of the ellipse. This comparison demonstrates whether edge loading can occur in the design. By subtracting the radial shifts from the teeth addenda, one also can evaluate the reduction in the ideal contact ratio.

This model can evaluate performance tradeoffs where transmission weight and transmission life are competing objectives. Figs. 8 and 9 are dimensionless plots of contact shift as function of support shaft stiffness for a single stage transmission. The plots vary both the gear

and pinion shaft stiffnesses by the same percentage. The parametric study reduces the stiffnesses from the design values to show the effect of shaft stiffness on performance.

Fig. 8 is a plot of the radial contact shift on both the gear and the pinion. Fig. 9 is a plot of the tangential contact shift for the two gears. Both plots show the contact shift as a ratio to the mid-cone base pitch of the teeth. This gives a dimensionless comparison of the shift magnitudes. A second vertical axis on the radial plot shows the shift as a percent of the tooth addendum. This compares the shift of the contact point to the actual tooth size. In the tangential shift plot, the second vertical axis shows the tangential shift as a percent of the half tooth width. The horizontal axis of both plots is the ratio of the support shaft stiffness, EI, to the full support shaft stiffness, EI_o.

The figures demonstrate a definite hyperbolic relationship between the stiffnesses and the resulting pitch point contact shift. A valuable conclusion is that one may reduce the stiffnesses in the example to about 20% of the nominal design values. At this point, there is a significant increase in the contact position shift. With this information available at the design stage of a transmission's development, important weight savings may be possible. The weight savings will not sacrifice the transmission's life or power overload performance seriously.

Summary and Conclusion

This article presents a method to predict the shift of the loaded region on the gear teeth in a spiral bevel reduction. This shift is a result of the elastic deflections of the gear support shafting and bearings under load. The reduction is a single spiral bevel gear drive with a pinion input and supporting shafts and bearings. The assumed deflections were caused by the shaft deflections, the shaft slopes, and the bearing deflections. The analysis assumed that the curvatures of the teeth near the pitch point were constant. It determined the curvatures using the envelope of cutting tool positions.

The analysis was sequential. The first stage defined the gear geometry and loading. The second stage determined the elastic deflections of the bearings and shafts and the slopes of the shafts at the gears. The third stage determined the motions of the gear teeth caused by each elastic deflection. Superposition of these motions produced the total deflections of the gear teeth. The fourth stage analyzed the interaction between the tooth geometry and motion to predict the tooth contact ellipse motions under load. A Fortran 77 computer program determined the radial and tangential tooth contact shifts of the gear and pinion.

An example representative of the main rotor bevel gear reduction found in the U.S. Army OH-58 helicopter was modelled. A parametric study illustrated the determination of the radial and tangential tooth contact ellipse shifts. Graphs showed the variation in contact shift with reduction in support shaft stiffness. An important conclusion was that, for the example, one could reduce the shaft stiffnesses to about 20% of the present stiffnesses. At this level, significant changes in the shifts of the tooth contact positions occurred. Significant weight reductions may be possible without seriously affecting the gear action or the gear life. ■

Acknowledgements: *Originally published as NASA Technical Memorandum 101438 and in the Proceedings of the ASME Fifth International Power Transmission and Gearing Conference 1989.*

References:

1. WILDHABER, E. "Basic Relationships of Bevel Gears." *American Machinist*. 1945. Vol. 89, No. 20,21,22; pp. 99-102, 118-21, 122-25.
2. WILDHABER, E. "Basic Relationships of Hypoid Gears." *American Machinist*. 1946. Vol. 90, No. 4, 5, 12, 13, 15, 16, 17; pp. 108-11, 131-4, 132-5, 110-4, 150-2, 106-10, 104-6, 122-8.
3. BAXTER, M.L., JR. "Basic Geometry and Tooth Contact of Hypoid Gears." *Industrial Mathematics*. Vol. 11, Pt. 2, pp. 19-42.
4. COLEMAN, W. "Guide to Bevel Gears." *Product Engineering*. 1963, pp. 87-95.
5. LITVIN, F.L. & COY, J.J. "Spiral Bevel Gear Geometry and Gear Train Precision." NASA CP 2210, 1981, pp. 335-344.
6. LITVIN, R.L., RAHMAN, P. & GOLDRICH, R.N. "Mathematical Models for the Synthesis and Optimization of Spiral Bevel Gear Tooth Surfaces." 1982, NASA CR 3553.
7. COLEMAN, W. "Analysis of Mounting Deflections on Bevel and Hypoid Gears." 1975. SAE Paper 750152.
8. TAHA, M.M.A., ETTLES, C.M., & MACPHERSON, P.B. "The Rigidity and Performance of a Helicopter Gearbox with a Cantilevered Housing and Two Taper Roller Bearings." *Journal of Mechanical Design*. 1978. Vol. 100, No. 6, pp. 696-702.
9. WINTER, H. & PAUL, M. "Influence of Relative Displacements Between Pinion and Gear on Tooth Root Stresses of Spiral Bevel Gears." *Journal of Mechanisms, Transmission, and Automation in Design*. 1985, Vol. 107, No. 3, pp. 43-48.
10. HARRIS, T.A. *Rolling Bearing Analysis*. 2nd. ed. John Wiley & sons, 1984.
11. HOUGHTON, P.S. *Ball and Roller Bearings*. Applied Science Publishers, 1976.
12. ROARK, R.J. & YOUNG, W.C. *Formulas for Stress and Strain*, 5th ed. McGraw-Hill, 1975.
13. ALTIDIS, P.C. & SAVAGE, M. "Flexibility Effects on Tooth Contact Location in Spiral Bevel Gear Transmissions." 1987, NASA CR-4055.